Hindawi
International Journal of Polymer Science
Volume 2022, Article ID 5970484, 12 pages
https://doi.org/10.1155/2022/5970484

Research Article

The Effect of Annealing on the Structure and Electric Performance of Polypropylene Films

Xiying Dai,[1] Zhaoliang Xing,[1] Wei Yang,[1] Chong Zhang,[1] Fei Li,[1] Xin Chen,[1] Chen Li,[2] Jianjun Zhou,[2] and Lin Li[2]

[1]*State Key Laboratory of Advanced Power Transmission Technology, Global Energy Interconnection Research Institute Co. Ltd., Beijing 102209, China*
[2]*Beijing Key Laboratory of Energy Conversion and Storage Materials, College of Chemistry, Beijing Normal University, Beijing 100875, China*

Correspondence should be addressed to Zhaoliang Xing; xingzhaoliang@geiri.sgcc.com.cn and Jianjun Zhou; 11112010101@bnu.edu.cn

Received 6 August 2022; Revised 7 September 2022; Accepted 9 September 2022; Published 8 November 2022

Academic Editor: Zhi Li

Biaxially oriented polypropylene (BOPP) and uniaxially oriented polypropylene (UOPP) films were annealed. The effect of annealing temperature (T_a) on dielectric strength was studied. The electric breakdown strength (E_b) of BOPP and UOPP films changes in a quite different trend with the annealing process. E_b of BOPP films decreases with the increase in T_a, whereas E_b of UOPP films increases first and then decreases with T_a. The structural changes during annealing were investigated. The crystallinity rises with T_a, while the orientation degree and E_b show a similar trend with T_a. Although the crystallinity and crystal structure can affect E_b of polypropylene films, the orientation of chain segments has a much larger correlation with E_b. Our results indicate that the deterioration of the metallized BOPP film capacitor may originate from the orientation degree decrease of chain segments after experiencing high temperature.

1. Introduction

Biaxially oriented polypropylene (BOPP) thin films are widely used in metallized film capacitors due to their extremely low dielectric loss (0.02%) and high dielectric strength (720 kV mm^{-1}) [1–3]. Furthermore, metallized film capacitors have the properties of self-healing, which have promoted a wide application of metallized BOPP film capacitors in ultrahigh voltage flexible direct current (DC) power grid, high-speed railway, and new energy electric vehicles [4, 5]. Increasing the energy density and service temperature of metallized film capacitors is the endless pursuit of producers and customers [6, 7]. The energy density of the metallized film capacitor is determined by the dielectric constant and the electric breakdown strength (E_b) [8, 9]. The dielectric constant at a specific frequency and temperature is hard to be improved since the dipole or polarization is the intrinsic properties of polypropylene, while E_b can be affected by the processing parameters during BOPP manufacturing. E_b can be modified by changing the thickness, crystallinity, and tensile strength of BOPP films [10]. E_b can also be improved with a higher biaxially stretching ratio [11].

When the metallized BOPP film capacitor experiences excessive voltage above E_b, a point defect short circuit between metallized electrodes of the capacitor can occur. The metallic layer of electrodes evaporates rapidly due to arc discharge together with localized high temperature. The elevated temperature will considerably reduce the lifetime expectancy of metallized polymer film capacitors [12]. Thermal aging is one of the main failure mechanisms in polymeric film capacitors [13, 14]. Most studies concentrated on the aging of metallized film capacitors at a high temperature by monitoring the changes in their basic parameters [15, 16]. Capacitance and equivalent series resistance were monitored as the parameters that reflect the aging process [17, 18]. Basically, some of the parametric changes can be

traced from the structure variation of the BOPP film [19]. However, although the performance of polypropylene (PP) capacitors during aging has been studied carefully, the structure evolution of the BOPP film during aging is not clearly investigated, which can be studied by annealing the BOPP film separately [20].

Annealing is an important process to modify the performance of plastics. During annealing, the oriented chain relaxes accompanied with the re-arrangement of chain segments, resulting in a variation of the structure and performance. A uniaxially oriented polypropylene (UOPP) film is a base film for preparing microporous films by stretching. To prepare microporous film with uniform pore size, the UOPP film should be annealed first to modify the crystallinity and orientation degree before stretching. Some studies showed that both the orientation degree and crystallinity increased with annealing temperature (T_a) [21, 22]. After annealing, the content of defects in crystals was decreased, the orientation of the crystalline phase was increased, and microcrystals formed in the amorphous between primary lamellae [23]. While some proposed that the amorphous part could be divided into mobile amorphous fraction and rigid amorphous fraction. Annealing promoted the formation of looser mobile amorphous fraction and more rigid amorphous fraction by the microstructural re-arrangement [24]. Although there were some studies investigating the structure evolution of annealing on UOPP film, few studies concentrated on the annealing behavior of produced BOPP film. While the structure change after annealing is vital to understand the performance deterioration of metallized BOPP film capacitor. Also, no one has ever studied the dielectric and electric breakdown properties of UOPP film. Although both BOPP and UOPP are oriented films, various manufacturing art has endowed the two kinds of films with different crystal structures. The influence of crystal structures on the dielectric properties of polypropylene has been investigated a lot. However, the differences of oriented crystal structures between BOPP and UOPP, as well as the primary factor of the oriented crystal structures on impacting the breakdown strength have not been well studied.

In this article, two kinds of oriented PP films were annealed at various temperatures, and studies were carried out to reveal the relationship between structure and dielectric strength. It is expected that our results can provide guidance for understanding the performance variation of metallized film capacitor.

2. Experimental Section

BOPP films with a thickness of 8 μm were obtained from Tongfeng Electronics (Tongling, China). The BOPP films were commercial products for metalized PP film capacitors. UOPP films with a thickness of 16 μm were obtained from Cangzhou Mingzhu Plastic Co. Ltd. (Cangzhou, China). The UOPP films were prepared by melt casting at a large die draw ratio with the properties of hard elastic, which could be used as base films for preparing uniaxially stretched PP microporous films. BOPP and UOPP films were rolled to anneal at 100–150°C for 1 hour before further characterized, which simulated the state when PP films were rolled in the capacitors.

The dielectric properties were measured using an impedance analyzer (Concept 40, Novocontrol GmbH, Montabaur, Germany) at room temperature from 10^7 to 10^2 Hz. E_b was conducted on the Dielectric Withstand Voltage Test System (Beiguang Jingyi Instrument Equipment Co., Ltd, Beijing, China). The leakage current was measured by a combination of power supply (Keithley, 2290-10) and System SourceMeter™ (Keithley, 2635B). The films were tested in insulating oil at room temperature. The two-parameter Weibull distribution was employed to analyze the DC breakdown strength of samples from the experimental data.

Differential scanning calorimetry (DSC) measurements were taken with a DSC (PerkinElmer, DSC 8000) at 10°C minute^{-1}. Indium and tin were employed for the temperature calibration. Samples of ~3.0 mg were sealed in aluminum pans and a nitrogen gas purge with a flux of ~20 mL minute^{-1} was used to prevent oxidative degradation of samples during the heating run. The crystallinity was calculated using the following equation:

$$X_c = \frac{\Delta H_f}{\Delta H_f^o}. \quad (1)$$

where ΔH_f is the melting enthalpy of α form crystals, ΔH_f^o (165 J g^{-1}) is the standard melt enthalpy of α form crystals.

Wide-angel X-ray diffraction [WAXD; Phillips X'pert Pro MPD diffractometer with Cu–Kα ($\lambda = 0.15418$ nm)] was further used to characterize the crystal form and crystallinity. The 2θ scanning range was 10–30° with the rate of 3 min^{-1}. The overall crystallinity, X_c, was calculated according to the following equation [25]:

$$X_c = \frac{\sum A_{cryst}}{\sum A_{cryst} + \sum A_{amorp}}, \quad (2)$$

where A_{cryst} and A_{amorp} are the fitted areas of crystal and amorphous regions, respectively.

Small-angle X-ray scattering (SAXS) was performed at 4B9A, Beijing Synchrotron Radiation Facility (BSRF), using a Mar345 detector. The sample was mounted onto a stage at the beamline at a sample to detector distance of 1750 mm. The one-dimensional correlation function $K(z)$ can be derived from the scattering intensity distribution profile as follows [26–28]:

$$K(z) = \frac{\int_0^\infty I(q) \cos(qz) dq}{\int_0^\infty I(q) dq}. \quad (3)$$

where z denotes the drawing direction. It must be noted that no multiplication q^2 to $I(q)$ is performed because of the highly anisotropic orientation of the lamellar crystals in the sample investigated and no extension of $I(q)$ to a higher angle is carried out.

Fourier transform infrared spectroscopy (FTIR) was applied to characterize the orientation degree of the PP films

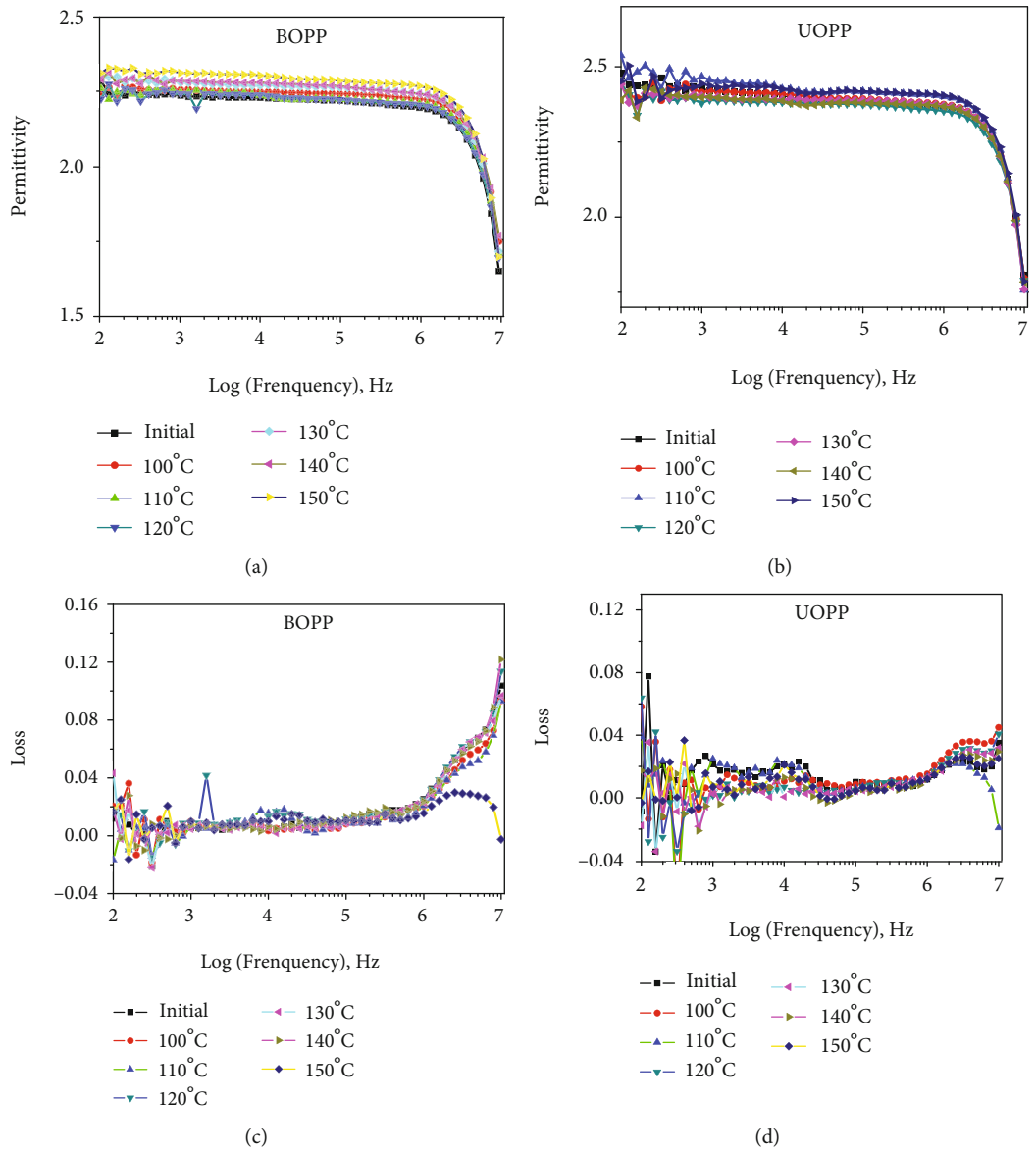

Figure 1: Permittivity and dielectric loss of the PP films. Permittivity of (a) BOPP and (b) UOPP. Dielectric loss of (c) BOPP and (d) UOPP.

according to the dichroic ratio D [29].

$$D = \frac{A_{//}}{A_{\perp}}, \tag{4}$$

where $A_{\parallel}$ is the absorption parallel and $A_{\perp}$ is the absorption perpendicular to a specific reference axis at a specific wavenumber. The Herman orientation function of this vibration is obtained according to [29]:

$$f = \frac{2}{3\cos^2\alpha - 1} * \frac{D-1}{D+2}. \tag{5}$$

where α is the angle between transition moment and polymer chain axis, and the α value of 18° was used. The orientation of the crystalline phase, f_c, can be determined from the D at 998 cm^{-1}. While the average orientation function, f_{av}, is obtained from the D at 972 cm^{-1}. The orientation of amorphous phase, f_a, is calculated according to:

$$f_{av} = X_c f_c + (1 - X_c) f_a, \tag{6}$$

where X_c is the degree of crystallinity determined by WAXD.

3. Results and Discussion

3.1. Dielectric Properties. The dielectric properties of BOPP and UOPP films are shown in Figure 1. It can be observed that the dielectric constants of BOPP and UOPP films are almost constant (~2.25 and 2.45, respectively) when the frequency is lower than 1×10^6 Hz, and the losses are <0.02%, suggesting that PP films are superior stable dielectrics. The permittivity and dielectric loss of homogeneous materials are mainly related to the dipole moment of materials [30,

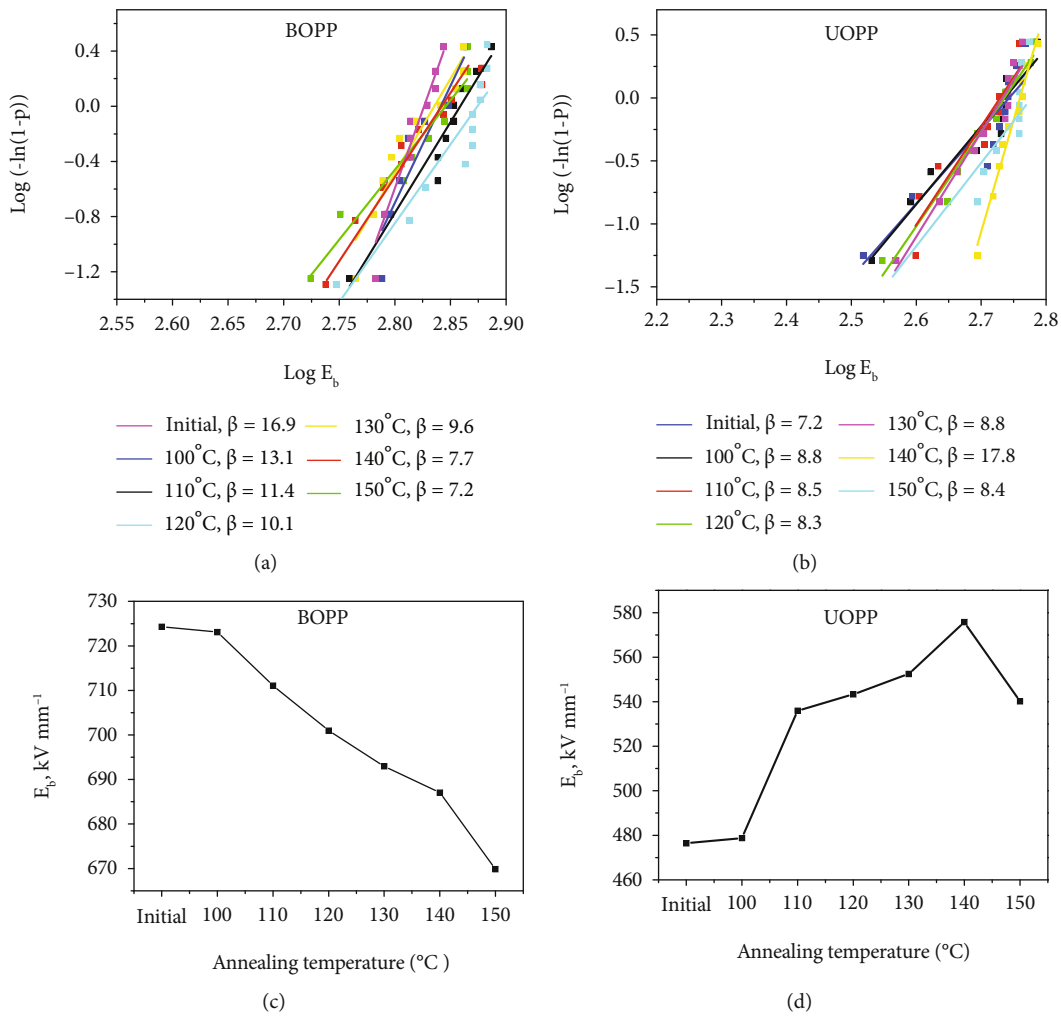

Figure 2: Weibull distribution and the E_b of PP films. Weibull distribution of (a) BOPP films and (b) UOPP films. E_b of (c) BOPP films and (d) UOPP films.

31]. Therefore, it is reasonable that the manufacturing method and annealing have no obvious effect on the dielectric constant and loss.

3.2. Electric Breakdown Strength. The electric breakdown strength of PP films was determined and fitted with a two-parameter Weibull distribution function: $P(E) = 1 - \exp(-(E/E_b)^{\beta})$, where $P(E)$ is the cumulative probability of the electric breakdown failure, E is the experimental electrical strength, E_b is the scale parameter, which means the breakdown strength at a cumulative failure probability of 63.2% and can be referred to as the characteristic breakdown strength of the dielectrics. The shape parameter β shows the dispersion of E data and the quality of film dielectrics [32, 33]. Figures 2(a) and 2(b) show the Weibull distribution of the PP films. The shape parameters β are about 10.0 and 8.5 for the BOPP films and UOPP films, respectively, suggesting a narrow dispersion of E data. Figures 2(c) and 2(d) show the E_b of PP films at different T_a. The E_b of initial BOPP film is 724.9 kV mm^{-1}. After annealed at 100°C for 1 hour, there is no obvious change in the E_b. When T_a is increased to 110°C, E_b decreases to about 712.5 kV mm^{-1}. Further increasing T_a leads to a gradual decrease of E_b. When T_a is higher than 140°C, an obvious decrease in the E_b can be observed. It can be concluded that E_b decreases with T_a for the BOPP films. For the UOPP films, quite different trend is observed. The E_b of initial UOPP film is 478.4 kV mm^{-1}, much lower than that of initial BOPP film. After annealed at 100°C for 1hour, E_b increases to about 480.8 kV mm^{-1}. Further increasing T_a leads to a gradual increase of E_b to 578.7 kV mm^{-1}. When the T_a is higher than 140°C, an obvious decrease in the E_b can also be observed. The obvious decrease of E_b in both kinds of PP films can be attributed to the partial melting of PP crystals at temperature higher than 140°C. When T_a is lower than 140°C, E_b of the BOPP film decreases with the increase in T_a, while that of UOPP film shows a quite different trend. The different effects of annealing on E_b should originate from different microstructure evolutions.

3.3. Thermal Analysis. The PP films were characterized with DSC as shown in Figure 3. The initial BOPP film has two melting peaks, one at 164.5°C and the other at 170.9°C as

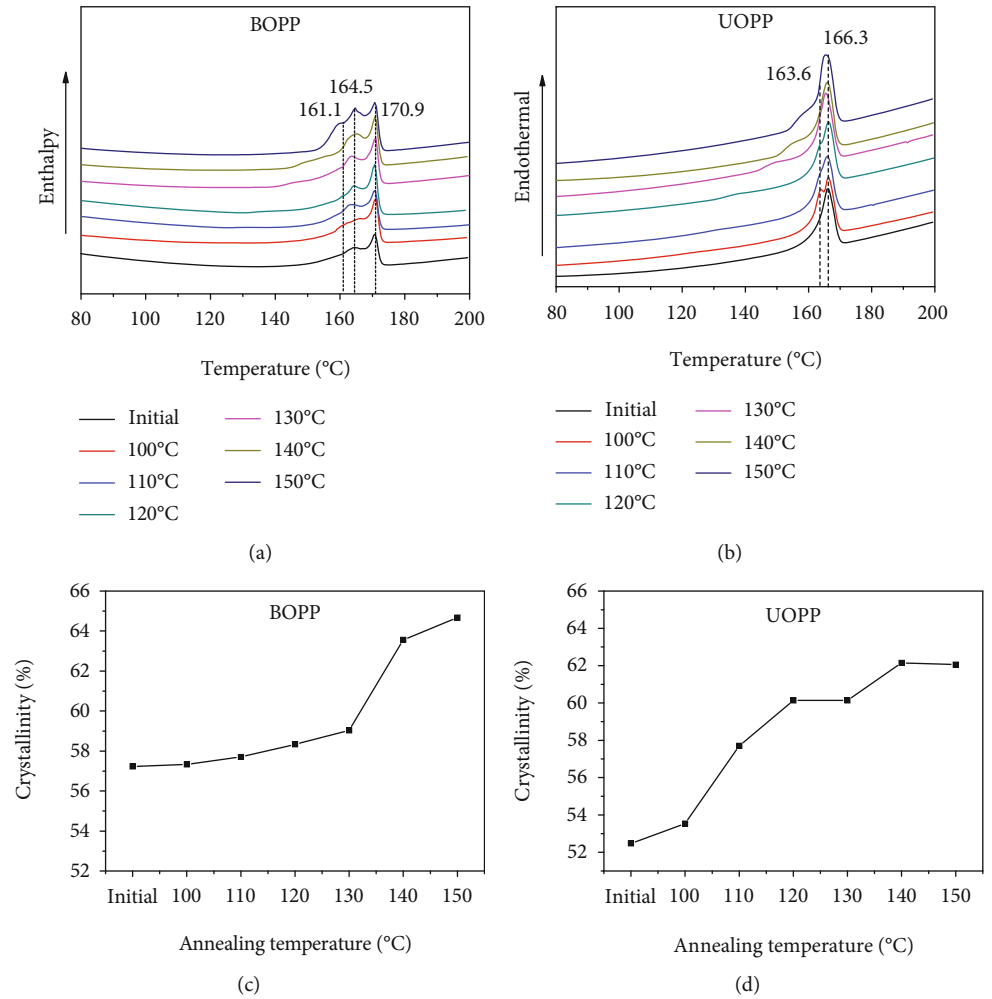

Figure 3: DSC heating curves and crystallinity of PP films. DSC heating curves of (a) BOPP films and (b) UOPP films. Crystallinity of (c) BOPP films and (d) UOPP films ($\Delta H_f^0 = 165\,J\,g^{-1}$).

shown in Figure 3(a). As the BOPP film was annealed at 100°C, a shoulder peak appears at 161.1°C, which gradually shifts to higher temperature and merges with the peak at 164.5°C at higher T_a. The shoulder peaks at about 161.1°C can be attributed to the melting of crystals formed at T_a, since they increase with T_a. While the peak at 164.5°C can be assigned to the melting of crystals from recrystallization. The peak at 170.9°C is much higher than the melting point of α form PP crystals (~163–167°C), which does not shift with T_a. Therefore, it is supposed that this melting peak should originate from the crystals with special microstructure. The industrially produced BOPP films have been stretched at large ratios (5.0 × 8.0) with the heat setting process to control the film shrinkage ratio. Therefore, there should exist a more stable microstructure that cannot be affected during the DSC heat scan. When polymers were stretched at a large ratio, fibril crystals may form. Different from the folding chain crystals, the fibril crystals have the properties of extend chain crystals with a melting point approaching the equilibrium melting point. The equilibrium melting point of PP α form crystal is ~186°C [34]. As a result, it is deduced that the peak at 170.9°C may be attributed to the melting of fibril crystals with partially extended chain segments [35]. Estimated from the proportion of the peak at 170.9°C, it is supposed that a large number of fibril crystals exist in BOPP films due to high ratio stretching in the manufacturing process.

The UOPP films show quite different thermal behavior from that of BOPP films as shown in Figure 3(b). The initial UOPP film has a melting peak at 166.3°C. After the UOPP film was annealed at 100°C, another melting peak appears at 163.6°C. Meanwhile, the melting peak at 163.6°C shifts to higher temperature and merges with the peak at 166.3°C, forming a shoulder peak on the left. According to the mechanism of lamellar thickening during high temperature annealing, the higher the T_a, the thicker the lamellae, the higher the melting temperature. The shoulder peak on the left side should originate from melting crystals formed at T_a, which may be attributed to the microcrystal form in the amorphous between the primary crystals [23]. For all UOPP films, the melting peak at 166.3°C does not change with the T_a. Since melting and recrystallization can easily take place during heating, the peak at 166.3°C may be attributed to the melting of crystals from recrystallization [36]. To

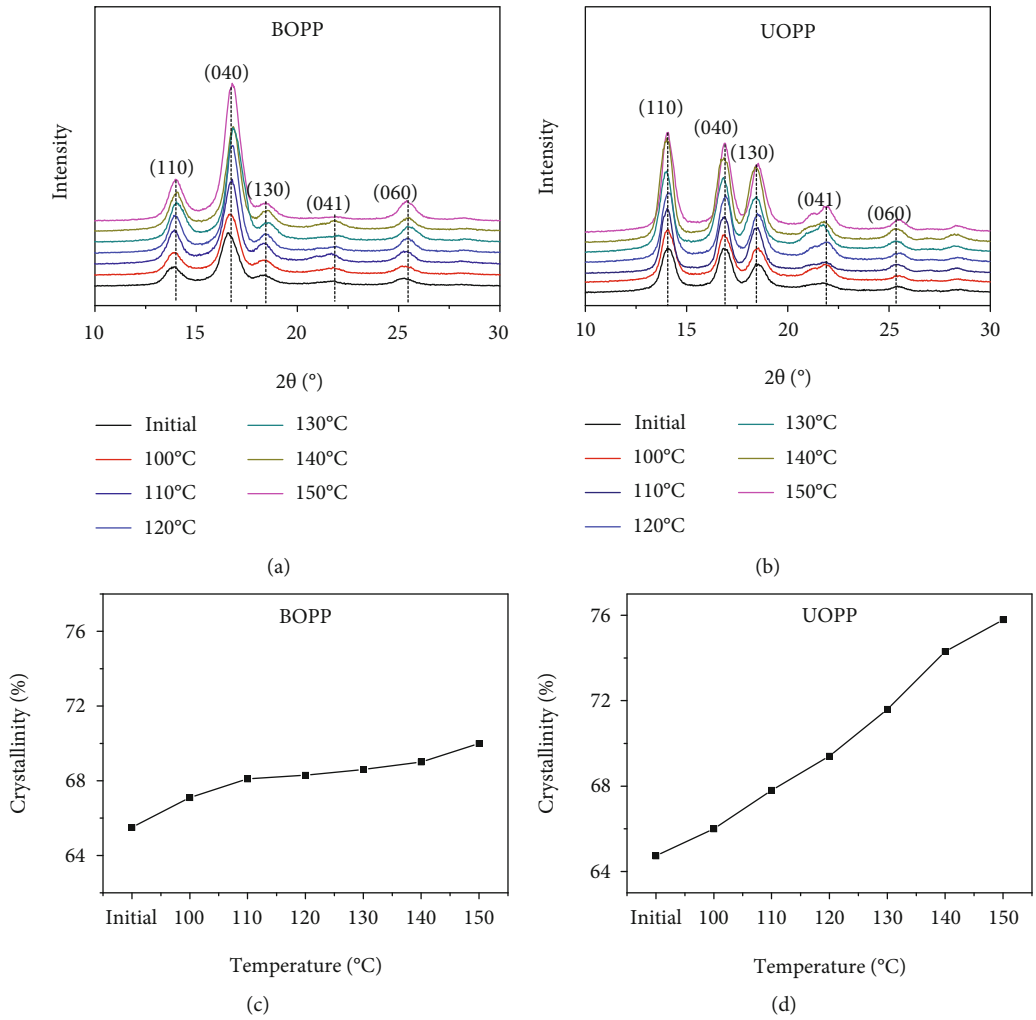

Figure 4: WAXD profiles and crystallinity of PP films. WAXD profiles of (a) BOPP films and (b) UOPP films. Crystallinity of (c) BOPP films and (d) UOPP films.

make sure that the different melting behavior is due to various manufacturing processes but not the raw material, the second DSC heating scan for both BOPP and UOPP were carried out. As shown in Figure S1, after eliminating thermal history, both PP resins show two melting peaks, that is, one at 148.7°C, another at 163.3°C, which indicates that PP resin with similar chain structure and composition has been used, and the different melting behavior of BOPP and UOPP films is originated from the difference in the manufacturing process.

The crystallinity was calculated using the melting enthalpy. The crystallinity of the initial BOPP film is 57.2%, which does not change when annealed at 100°C. As T_a is higher than 100°C, a gradual increase in crystallinity with T_a is observed, which changes greatly as the temperature is higher than 140°C. The highest crystallinity reaches 64.7% when annealed at 150°C. The crystallinity of initial UOPP film is about 52.5%. A large increase is observed as T_a is 110°C, and the highest crystallinity is 62.0% when annealed at 150°C. The crystallinity of the UOPP films is low, and it increases in a different manner compared with the BOPP films, which can be attributed to different manufacturing processes.

3.4. Wide-Angel X-Ray Diffraction. Figures 4(a) and 4(b) show the WAXD profiles of the PP films. The peaks at 2θ angles of 14.1, 16.9, 18.6, and 25.7° can be assigned to the reflection peaks of (110), (040), (130), and (060) of α-form, respectively. The crystallinity was calculated after separating the amorphous phase, and the results are shown in Figures 4(c) and 4(d). The crystallinity of both kinds of films increases with T_a. For BOPP films, the crystallinity of the initial film is about 65.5%. The highest crystallinity of 70.0% is obtained at 150°C. While for UOPP films, the crystallinity of the initial film is about 64.7%, lower than that of BOPP film. The values increase sharply with T_a. The highest crystallinity of 75.8% is obtained at 150°C. The crystallinity obtained by DSC and WAXD shows the same trend of increasing with T_a, but in a different manner. Melting and recrystallization during the DSC heating scan may be the factor leading to the difference. When comparing Figure 2(c) with Figure 4(c), it can be observed that the crystallization and E_b of BOPP films change in an opposite trend. The initial BOPP film has the highest E_b, while the crystallinity is the lowest. After annealing at 100°C, slightly decreased E_b with a slightly increased crystallinity is

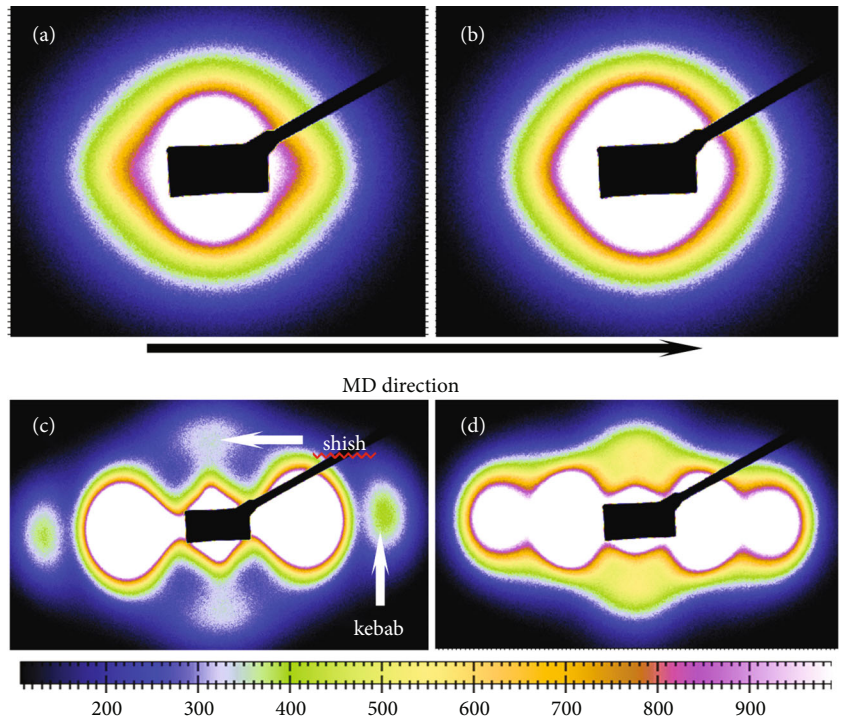

Figure 5: Small-angle X-ray scattering patterns of the PP films: (a) initial BOPP film, (b) BOPP film after annealed at 130°C, (c) initial UOPP film, and (d) UOPP film after annealed at 130°C.

observed. The slightly increase in crystallinity may be due to the relaxation and crystallization of low-molecular-weight fraction. As T_a is in the range of 110–140°C, E_b declines gradually, while the crystallinity increases slowly. The increase in T_a may have resulted in the partial melting and recrystallization, leading to the re-organization of crystals. As T_a is 150°C, a temperature near the melting point, the melting recrystallization and crystal re-organization should be more intense during annealing, and E_b decreases sharply. The comparison implies that the crystal structure change due to annealing will weaken the E_b of BOPP film. When comparing Figure 2(d) with Figure 4(d), both E_b and crystallinity of UOPP films increase with T_a, as T_a is lower than 140°C, which suggests that annealing favors strengthening the E_b of the UOPP film. As T_a is 150°C, the crystallinity reaches the highest, while E_b also decreases sharply, indicating the collapse of oriented crystal structure. The E_b and crystallinity of BOPP and UOPP films change in different ways with T_a, which suggests that crystallinity is not the determining factor affecting E_b.

3.5. Small-Angle X-Ray Scattering. SAXS was used to explore the effect of annealing on the microstructure of PP films. The typical 2D SAXS pattern of the BOPP and UOPP initial films are displayed in Figure 5. The initial BOPP film has an oblate pattern, indicating that the orientation in the traverse direction is larger than the machine direction (MD). After annealing at 130°C, there is no significant change in the shape of the SAXS pattern when compared with the diagrams of initial films, whereas the UOPP film shows a typical uniaxial orientation pattern. The weak meridional streak in SAXS patterns is attributed to the shish-like crystals such as extended chain crystal structures and row nuclei in MD, while the appearance of strong equatorial maxima is attributed to kebab-like lamellar stacks, oriented perpendicularly to the MD [37]. After annealing at 130°C, the scattering intensity of both the shish-like and kebab-like crystals increases obviously. The morphologies of both BOPP and UOPP films after annealed at 130°C were observed with atomic force microscopy as shown in Figure S2. Crystals with no obvious orientation are observed in the BOPP film [Figure S2(a)], while parallel lamellar stacks are seen in the UOPP film [Figure S2(b)], which accords well with the 2D SAXS pattern.

The one-dimensional scattering intensity distributions of the BOPP films along the MD direction are shown in Figure 6(a). A much stronger increase in intensity is observed as T_a is higher than 130°C, indicating crystal perfection with the increase of the electron density difference between the lamellar crystals and amorphous layers. The one-dimensional correlation function derived from the scattering intensity distribution profile is shown in Figure 6(c). When the crystallinity is larger than 50%, the average thickness of the amorphous layer (d_a) and long period of lamellar stacks (d_{ac}) can be directly obtained from the correlation function [Figure 6(c)] [27]. The average d_a, d_{ac}, and average thickness of crystals (d_c) values of BOPP films are shown in Figure 6(e). The initial d_a, d_c, and d_{ac} values of the initial BOPP film are 4.2, 13.9 and 18.1 nm, respectively, which keeps almost stable as T_a is lower than 120°C. Obvious lamellar thickening appears as T_a is higher than 120°C, which can be attributed to the partial melting of unstable crystals followed by the structural re-organization during annealing at high temperatures.

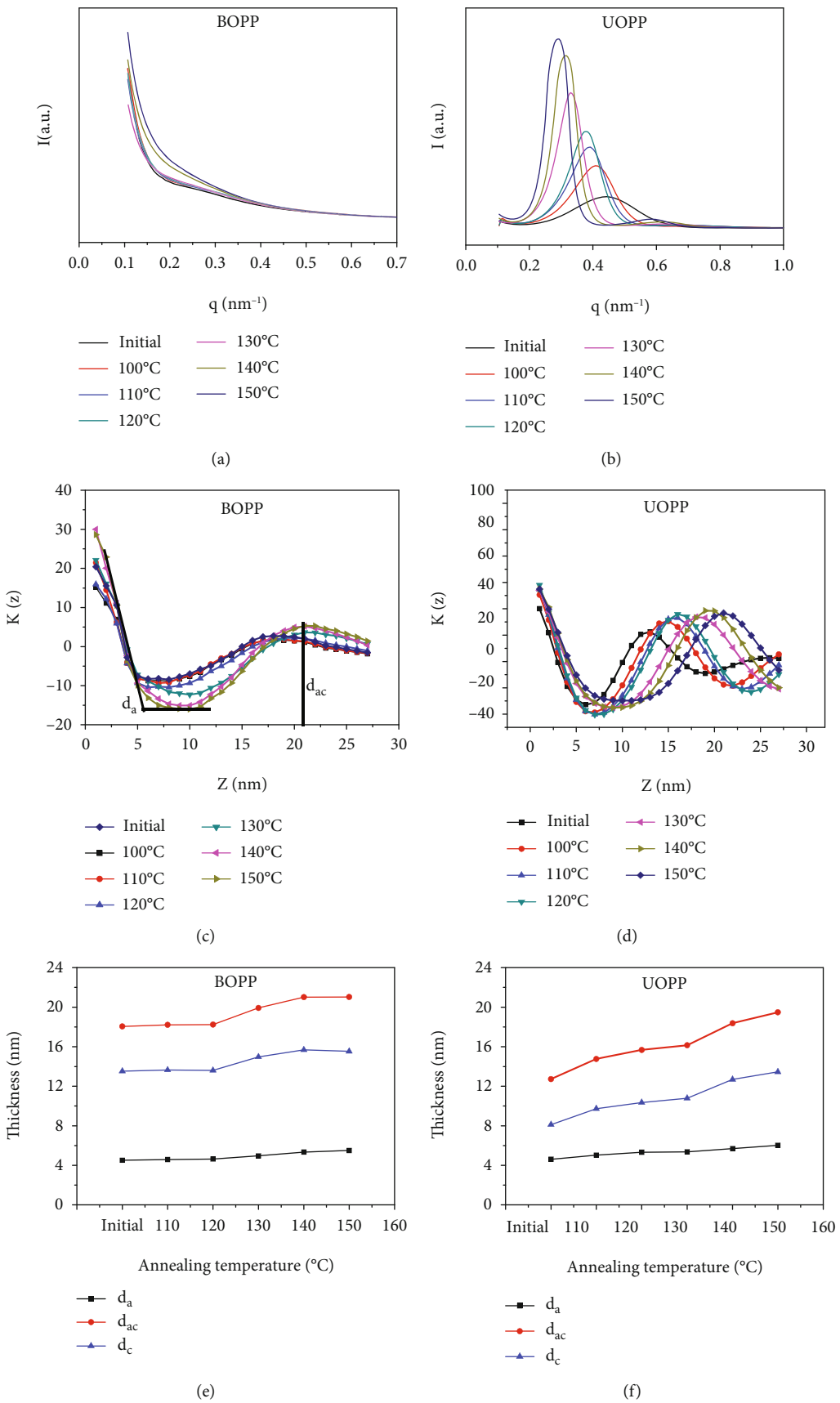

Figure 6: One-dimensional scattering intensity distribution profiles taken along the MD direction (a) and (b), the corresponding correlation functions (c) and (d), long periodicity, lamellar thickness, and the average thickness of the amorphous layer (e) and (f) at different annealing temperatures.

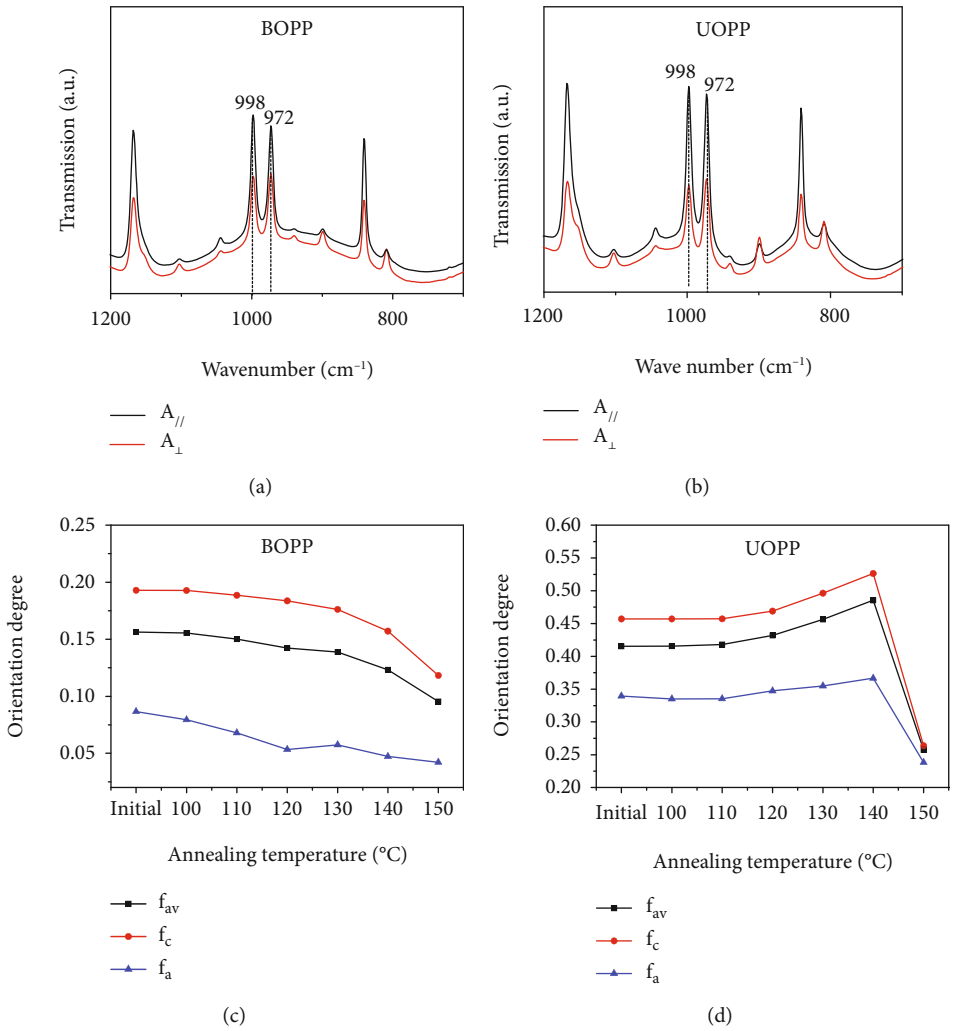

FIGURE 7: Polarized FTIR spectra of (a) BOPP and (b) UOPP films. Changes in the orientation function with T_a for (c) BOPP and (d) UOPP films.

The one-dimensional scattering intensity distributions of UOPP films along the MD direction are shown in Figure 6(b). It can be observed that the scattering peak shifts to smaller scattering vector q values with stronger intensity with the increase in T_a, which is the evidence of crystal perfection with the re-arrangement of lamellae and/or amorphous parts, resulting in an increase of the long periodicity and the electron density difference between the lamellar crystals and amorphous layers. The resultant correlation functions are shown in Figure 6(d). The average d_a, d_c, and d_{ac} values of UOPP films are shown in Figure 6(f). Compared with the initial UOPP film, all the thicknesses increase with the increase in T_a. The increase in thickness can be assigned to volume expansion, the crystallization of amorphous part and re-organization of lamellar crystals by lamellar thickening. Compared with d_a, d_c and d_{ac} increase in a much higher rate, especially when T_a is higher than 130°C, suggesting the lamellar thickening with the rise of T_a. The average d_a values of both the initial UOPP and BOPP films are at the same level, while the d_c values are quite different, which can be attributed to the different film manufacturing process. The initial UOPP film is prepared using high-speed melt elongation, followed by quenching, resulting in imperfect crystals with small d_c (~8.1 nm). While the BOPP film is made by biaxially stretching followed by heat setting near the melting temperature, high temperature heat setting leading to more stable crystals with much higher d_c (~13.9 nm). The initial size and stability of the crystals in the initial films are quite different, so annealing has different effects on the structure evolution of two kinds of PP films. The d_c increases with T_a, while E_b varies in a different trend [Figures 2(c) and 2(d) and 6(e) and 6(f)], which implies that long period of lamellar stacks or lamellar thickness variation cannot be directly correlated with E_b.

3.6. Fourier Transform Infrared Spectroscopy. The polarized FTIR spectra of polypropylene are shown in Figures 7(a) and 7(b). The absorption at the wavenumber of 998 cm^{-1} is attributed to the crystalline phase (c-axis) while absorption at the wavenumber of 972 cm^{-1} is due to the contribution of both crystalline and amorphous phases [38]. The Herman orientation function was calculated according to the dichroic

ratio as shown in Figures 7(c) and 7(d). For the BOPP films, f_c decreases slowly while f_a decreases fast with the rise of T_a first, which suggests that the amorphous chain segments relax faster than those in the crystal. As T_a is higher than 130°C, f_c reduces in a much rapid rate, indicating reorganization of crystals. For the UOPP films, f_c and f_a almost keep stable below 110°C. As T_a is further increased, the orientations of the amorphous part and the crystal increase. Since the UOPP film consists of shish-kebab lamellae, that is, minor shish-like crystals growing along MD and a large number of kebab-like crystals oriented along the traverse direction, the increase in the orientation degree indicates that chain segments pack along MD during the lamellar reorganization. As T_a is higher than 140°C, the orientation degree falls down suggesting the collapse of the uniaxial orientation structure, which should be the upper limit application temperature for the UOPP film. When comparing Figure 2(c) with Figure 7(c), it can be observed that the initial BOPP film has the highest E_b and orientation degree. As T_a is increased to a temperature lower than 120°C, f_a declines faster than, which may suggest that the decrease of E_b may mainly originate from the decrease of f_a. As T_a is further increased to temperature lower than 140°C, f_c declines faster than f_a, implying the decrease of E_b may be due to the relaxation of f_c as a result of melting and recrystallization. As T_a is 150°C, f_c declines sharply, indicating obvious melting has led to the structure collapse of BOPP film, so E_b has the lowest value. For the UOPP film, both f_c and E_b increase with T_a, as T_a is lower than 140°C. As T_a is 150°C, both f_c and E_b fall. The orientation degree of both BOPP and UOPP films can correlate with E_b very well, suggesting that the orientation degree is highly correlated with the E_b of PP films. But linear correlation is not observed (Figure S1), since the crystallinity also has great influence on E_b [39]. Uniaxial orientation endows larger anisotropy to the films than biaxial orientation (Figure 5), so it seems that orientation degree is not feasible for comparison between different types of PP films. BOPP film has been stretched at large ratios (5.0×8.0) at both MD and traverse direction. Although the orientation degree of BOPP film is smaller, the chain segments orientation should be much larger than those of the UOPP film. E_b of BOPP film is much larger than that of UOPP film [Figures 2(c) and 2(d)], suggesting that microscopic chain segment orientation plays a more important role in E_b than the macroscopic orientation of lamellar stacks. Due to much higher E_b, BOPP film is the best choice for metallized PP film capacitor. When metallized PP film capacitor is thermally aged or self-healing after locally electric breakdown, the performance deterioration may result from chain segment re-organization, especially the decrease in orientation degree after experiencing high temperature.

4. Conclusion

BOPP and UOPP films were annealed, and the electric performance and structure evolution had been investigated. The BOPP films have high initial E_b, which decreases with T_a. The UOPP films have low initial E_b, which increases first and then decreases with T_a. In BOPP films, there exist a large number of fibril crystals with larger lamellar thickness and higher melting temperature. While in UOPP films, folded chain crystals are the main crystal species. The crystallinity of both films rises with T_a, and obvious lamellar thickening takes place after 130°C. The orientation degree and E_b show similar trend with T_a for both BOPP and UOPP films, suggesting that orientation degree is highly correlated with the E_b. Higher E_b of BOPP films can be attributed to larger lamellar thickness and higher orientation of chain segments. The performance deterioration of metallized PP film capacitors after aging or experiencing local high temperature may result from the decrease in the orientation degree of the BOPP film.

Data Availability

Data are presented in the supplementary information files.

Conflicts of Interest

The authors declare that they have no conflicts of interest.

Acknowledgments

This study was supported by the State Key Laboratory of Advanced Power Transmission Technology (Grant No. GEIRI-SKL-2020-009).

Supplementary Materials

The orientation degree is plotted with electric breakdown strength. *(Supplementary Materials)*

References

[1] J. L. Nash, "Biaxially oriented polypropylene film in power capacitors," *Polymer Engineering and Science*, vol. 28, no. 13, pp. 862–870, 1988.

[2] J. Ho and T. R. Jow, "High field conduction in biaxially oriented polypropylene at elevated temperature," *IEEE Transactions on Dielectrics and Electrical Insulation*, vol. 19, no. 3, pp. 990–995, 2012.

[3] E. W. Anderson and D. W. McCall, "The dielectric constant and loss of polypropylene," *Journal of Polymer Science*, vol. 31, no. 122, pp. 241-242, 1958.

[4] M. Ritamäki, I. Rytöluoto, and K. Lahti, "Performance metrics for a modern BOPP capacitor film," *IEEE Transactions on Dielectrics and Electrical Insulation*, vol. 26, no. 4, pp. 1229–1237, 2019.

[5] H. N. Nagamani and S. Ganga, "A study of electrical endurance of MPPF capacitors and selection of end-point criteria," *IEEE Transactions on Dielectrics and Electrical Insulation*, vol. 27, no. 6, pp. 1193–1201, 1992.

[6] B. J. Chu, X. Zhou, K. L. Ren et al., "A dielectric polymer with high electric energy density and fast discharge speed," *Science*, vol. 313, no. 5785, pp. 334–336, 2006.

[7] Q. Li, L. Chen, M. R. Gadinski et al., "Flexible high-temperature dielectric materials from polymer nanocomposites," *Nature*, vol. 523, no. 7562, pp. 576–579, 2015.

[8] X. Y. Huang and P. K. Jiang, "Core–shell structured high-*k* polymer nanocomposites for energy storage and dielectric

applications," *Advanced Materials*, vol. 27, no. 3, pp. 546–554, 2015.

[9] L. Zhu and Q. Wang, "Novel ferroelectric polymers for high energy density and low loss dielectrics," *Macromolecules*, vol. 45, no. 7, pp. 2937–2954, 2012.

[10] J. Y. Lu, B. F. Zhu, X. Zhang, and X. Wang, "Dielectric strength structure-activity relationship of BOPP film for high energy density pulse capacitor," *IEEE Transactions on Plasma Science*, vol. 47, no. 9, pp. 4342–4349, 2019.

[11] I. Rytoluoto, A. Gitsas, S. Pasanen, and K. Lahti, "Effect of film structure and morphology on the dielectric breakdown characteristics of cast and biaxially oriented polypropylene films," *European Polymer Journal*, vol. 95, pp. 606–624, 2017.

[12] H. Li, H. Li, Z. Li et al., "Temperature dependence of self-healing characteristics of metallized polypropylene film," *Microelectronics and Reliability*, vol. 55, no. 12, pp. 2721–2726, 2015.

[13] J. Hannonen, J. Honkanen, J. Ström, T. Kärkkäinen, S. Räisänen, and P. Silventoinen, "Capacitor aging detection in a DC–DC converter output stage," *IEEE Transactions on Industry Applications*, vol. 52, no. 4, pp. 3224–3233, 2016.

[14] H. M. Umran, F. Wang, and Y. He, "Ageing: causes and effects on the reliability of polypropylene film used for HVDC capacitor," *IEEE Access*, vol. 8, pp. 40413–40430, 2020.

[15] M. Makdessi, A. Sari, and P. Venet, "Metallized polymer film capacitors ageing law based on capacitance degradation," *Microelectronics and Reliability*, vol. 54, no. 9-10, pp. 1823–1827, 2014.

[16] M. Makdessi, A. Sari, P. Venet et al., "Lifetime estimation of high-temperature high-voltage polymer film capacitor based on capacitance loss," *Microelectronics and Reliability*, vol. 55, no. 9–10, pp. 2012–2016, 2015.

[17] W. J. Sarjeant, F. W. MacDougall, D. W. Larson, and I. Kohlberg, "Energy storage capacitors: aging, and diagnostic approaches for life validation," *IEEE Transactions on Magnetics*, vol. 33, no. 1, pp. 501–506, 1997.

[18] M. Teixeira, I. Del Hoyo, F. Wandrowelsti, V. Swinka-Filho, and M. Munaro, "Evaluation of thermal degradation in isotactic polypropylene films used in power capacitors," *Journal of Thermal Analysis and Calorimetry*, vol. 130, no. 2, pp. 997–1002, 2017.

[19] G. Wu, L. Zhou, X. Zhang, S. Bian, H. Ran, and C. Yu, "Study on the failure factors of composite insulation in high-voltage storage capacitors," *IEEE Transactions on Plasma Science*, vol. 38, no. 2, pp. 186–193, 2010.

[20] W. J. O'Kane, R. J. Young, and A. J. Ryan, "The effect of annealing on the structure and properties of isotactic polypropylene films," *Journal of Macromolecular Science, Part B: Physics*, vol. 34, pp. 427–458, 1995.

[21] F. Sadeghi, A. Ajji, and P. J. Carreau, "Analysis of microporous membranes obtained from polypropylene films by stretching," *Journal of Membrane Science*, vol. 292, no. 1-2, pp. 62–71, 2007.

[22] S. H. Tabatabaei, P. J. Carreau, and A. Ajji, "Microporous membranes obtained from polypropylene blend films by stretching," *Journal of Membrane Science*, vol. 325, no. 2, pp. 772–782, 2008.

[23] D. M. Liu, J. Kang, M. Xiang, and Y. Cao, "Effect of annealing on phase structure and mechanical behaviors of polypropylene hard elastic films," *Journal of Polymer Research*, vol. 20, no. 5, p. 126, 2013.

[24] H. W. Bai, F. Luo, T. N. Zhou, H. Deng, K. Wang, and Q. Fu, "New insight on the annealing induced microstructural changes and their roles in the toughening of β-form polypropylene," *Polymer*, vol. 52, no. 10, pp. 2351–2360, 2011.

[25] H. Huo, S. Jiang, L. An, and J. Feng, "Influence of shear on crystallization behavior of the β phase in isotactic polypropylene with β-nucleating agent," *Macromolecules*, vol. 37, no. 7, pp. 2478–2483, 2004.

[26] R. H. Somani, L. Yang, B. S. Hsiao, T. Sun, N. V. Pogodina, and A. Lustiger, "Shear-induced molecular orientation and crystallization in isotactic polypropylene: effects of the deformation rate and strain," *Macromolecules*, vol. 38, no. 4, pp. 1244–1255, 2005.

[27] G. Strobl, *The Physics of Polymers*, Springer, Berlin, 2nd ed. edition, 1997.

[28] L. Fu, Z. Jiang, H. F. Enderle et al., "Nature of molecular network in thermal shrinkage behavior of oriented high- density polyethylene," *Journal of Polymer Science Part B: Polymer Physics*, vol. 52, no. 5, pp. 368–376, 2014.

[29] S. H. Tabatabaei, P. J. Carreau, and A. Aji, "Structure and properties of MDO stretched polypropylene," *Polymer*, vol. 50, no. 16, pp. 3981–3989, 2009.

[30] H. Gao, C. Wang, Z. Yang, and Y. Zhang, "3D porous nickel metal foam/polyaniline heterostructure with excellent electromagnetic interference shielding capability and superior absorption based on pre-constructed macroscopic conductive framework," *Composites Science and Technology*, vol. 213, article 108896, 2021.

[31] C. Wang, H. Gao, D. Liang et al., "Effective fabrication of flexible nickel chains/acrylate composite pressure-sensitive adhesives with layered structure for tunable electromagnetic interference shielding," *Advanced Composites and Hybrid Materials*, 2022.

[32] J. Y. Jiang, X. Zhang, Z. K. Dan et al., "Tuning phase composition of polymer nanocomposites toward high energy density and high discharge efficiency by nonequilibrium processing," *ACS Applied Materials & Interfaces*, vol. 9, no. 35, pp. 29717–29731, 2017.

[33] T. Zhou, J. W. Zha, R. Y. Cui, B. H. Fan, J. K. Yuan, and Z. M. Dang, "Improving dielectric properties of $BaTiO_3$/ferroelectric polymer composites by employing surface hydroxylated $BaTiO_3$ nanoparticles," *ACS Applied Materials & Interfaces*, vol. 3, no. 7, pp. 2184–2188, 2011.

[34] K. Mezghani, R. A. Campbell, and P. J. Phillips, "Lamellar thickening and the equilibrium melting point of polypropylene," *Macromolecules*, vol. 27, no. 4, pp. 997–1002, 1994.

[35] R. H. Somani, L. Yang, I. Sics et al., "Orientation-induced crystallization in isotactic polypropylene melt by shear deformation," *Macromolecular Symposia*, vol. 185, no. 1, pp. 105–117, 2002.

[36] A. Menyhard, J. Varga, and G. Molnar, "Comparison of different-nucleators for isotactic polypropylene, characterisation by DSC and temperature-modulated DSC (TMDSC) measurements," *Journal of Thermal Analysis and Calorimetry*, vol. 83, no. 3, pp. 625–630, 2006.

[37] F. Sadeghi, A. Ajji, and P. J. Carreau, "Analysis of row nucleated lamellar morphology of polypropylene obtained from the cast film process: effect of melt rheology and process conditions," *Polymer Engineering and Science*, vol. 47, no. 7, pp. 1170–1178, 2007.

[38] J. Z. Xu, L. Xu, Y. Y. Liang, G. J. Zhong, J. Lei, and Z. M. Li, "Temperature dependence of molecular conformation in uniaxially deformed isotactic polypropylene investigated by combination of polarized FTIR spectroscopy and 2D correlation analysis," *Journal of Polymer Science Part B: Polymer Physics*, vol. 53, no. 9, pp. 673–684, 2015.

[39] C. Zhang, X. Y. Dai, Z. L. Xing et al., "Investigation on the structure and performance of polypropylene sheets and biaxially oriented polypropylene films for capacitors," *Chinese Journal of Polymer Science*, 2022.